

UNIVERSIDAD DE CANTABRIA

Facultad de Ciencias

Departamento de Física Aplicada



Tesis Doctoral

SYNTHESIS, STRUCTURAL CHARACTERIZATION AND  
SPECTROSCOPIC STUDY OF NANOCRYSTALLINE  
AND MICROCRYSTALLINE MATERIALS

Rosa Martín Rodríguez

Santander, Noviembre de 2010

# Chapter 3

## Synthesis

### 3.1 Introduction

In this chapter, the different synthesis methods used for the preparation of the samples are described.  $\text{Er}^{3+}$  and  $\text{Yb}^{3+}$  co-doped  $\text{Y}_2\text{O}_3$  and  $\text{NaYF}_4$  nanoparticles, as well as CdS nanopowders were prepared in a planetary ball mill at the Solid State Physics laboratory of the University of Cantabria. RE-doped  $\text{Y}_2\text{O}_3$  nanocrystals were also synthesized following a combustion reaction at the Inorganic Chemistry laboratory of our university.  $\text{Tb}^{3+}$ - $\text{Yb}^{3+}$  and  $\text{Eu}^{3+}$ - $\text{Yb}^{3+}$  co-doped ternary oxides GGG and YAG nanocrystalline samples, and  $\text{Cr}^{3+}$ -doped GGG nanoparticles were grown during a two month stay within Prof. Marco Bettinelli's group at the Biotechnology Department, University of Verona. All of them were obtained using Pechini's method [1]. Some of these samples were coated with  $\text{SiO}_2$  using Stöber method [2]. As another result of this collaboration, microcrystalline powders of LMA doped with  $\text{Mn}^{2+}$  and  $\text{Yb}^{3+}$  were also synthesized in one of Prof. Marco Bettinelli's laboratory. Colloidal  $\text{Zn}_{1-x}\text{Co}_x\text{O}$  nanocrystals were prepared at the Chemistry Department, University of Washington, thanks to a collaboration with Prof. Daniel R. Gamelin during a three month stay in his group.

### 3.2 Mechano-chemical processes in a planetary ball mill

A wide variety of processes such as crystallization of amorphous alloys, particle size reduction or mechano-chemical reactions can take place in a planetary ball mill [3]. In all

cases, mechanical ball milling consists of repeated fracture, mixing and welding of powder particles (less than  $10\ \mu\text{m}$  in size). When the mill rotates in one direction the vials rotate in the opposite one, and there are collisions among the powders, the balls and the vials walls [4]. The occurrence of these mechano-chemical reactions is attributed to the heat generated in the milling process, favored by the large area of contact between the solids [5]. At the point of collision, the solids deform and even melt, forming hot points where the molecules can reach very high vibrational excitation leading to bond breaking. Related to the final nanoparticles size, it is important to point out the existence of a steady-state grain size during high-energy ball-milling. If the initial size is bigger than the steady-state size, the crystallite size decreases during the milling, but smaller particles show an increase in size reaching finally such steady-state. This can be explained by an equilibrium between fracturing and crystal growth processes during the milling [6].



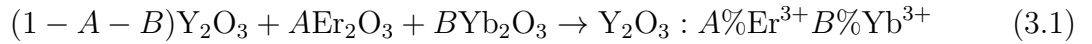
Figure 3.1: Planetary ball mill used for the synthesis of  $\text{Y}_2\text{O}_3$ ,  $\text{NaYF}_4$  and  $\text{CdS}$  nanoparticles at the Solid State Physics laboratory, University of Cantabria.

The high-energy ball-milling synthesis was carried out using a planetary ball mill (Retsch PM 400/2) (Fig. 3.1). The most important parameters to take into account in these processes are: Vials and balls material, balls size, atmosphere under which synthesis is performed (Air or argon), total milling time, milling and pause times, angular velocity (rpm), ball to sample mass ratio and the addition of a diluent. Changes in every parameter are decisive not only for the obtention of the desired phase but also for the final size of the nanocrystals. Searching for the optimum conditions for each synthesis process involved an arduous and systematic work. In some cases, the ball mill was also used in order to

homogenize the size of nanoparticles prepared using other synthesis methods.

### 3.2.1 Er<sup>3+</sup>, Yb<sup>3+</sup> co-doped Y<sub>2</sub>O<sub>3</sub>

Y<sub>2</sub>O<sub>3</sub>: Er<sup>3+</sup>, Yb<sup>3+</sup> nanoparticles were obtained in a planetary ball mill by intimately mixing stoichiometric quantities of yttrium, erbium and ytterbium oxides according to the reaction:

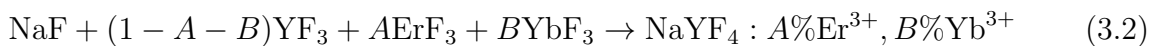


The following parameters were used:

- ZrO<sub>2</sub> vials and balls, with ball diameter of 10 mm. Other materials such as steel had been previously tried, but they contaminated the samples.
- Ball to powder mass ratio of 10:1, with a total amount of 6 g.
- Air atmosphere and 200 rpm.
- 5 minute stop every 30 minutes of milling. The dependence of the particle size on the total milling time was studied in order to determine the most advantageous conditions.

### 3.2.2 Er<sup>3+</sup>, Yb<sup>3+</sup> co-doped NaYF<sub>4</sub>

Different procedures have been previously described in the literature for the synthesis of sodium yttrium fluoride, NaYF<sub>4</sub>, such as heating the mixture NaF + YF<sub>3</sub> at 800 °C under HF gas [7] or a hydrothermal method that requires complicated apparatus [8]. These restrictions in fluoride synthesis have limited their development in comparison, for instance, with oxides. Fluorides have also been prepared by mechano-chemical synthesis [9]. This fact, and the difficulty in synthesizing the pure hexagonal phase by other methods, led us to prepare hexagonal NaYF<sub>4</sub>: Er<sup>3+</sup>, Yb<sup>3+</sup> nanocrystals using the planetary ball mill starting from stoichiometric quantities of fluorides according to the reaction:



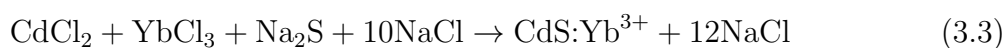
Bearing in mind the necessity of using parameters which increase collisions energy during the milling [9], it is convenient to increase the ball to powder mass ratio or the angular velocity. A systematic study to obtain the optimal synthesis conditions was accomplished; different grinding times, velocity and mass ratio were tried. The final parameters established as the most convenient for the synthesis of hexagonal NaYF<sub>4</sub> were:

- ZrO<sub>2</sub> vials and 20 balls.
- Ball to sample mass ratio of 30:1.
- Argon atmosphere and 300 rpm.
- 2 hours stop every grinding hour.

Different total milling times were used in order to get the pure hexagonal phase. Changes in any of the former parameters are rather critical for the obtention of the desired hexagonal phase. For example, if a ball to powder mass ratio of 20:1 is used, cubic phase is obtained after 5 hours milling. If a 5 minute pause is set, peaks corresponding to cubic phase are more intense than hexagonal peaks after 8 hours milling.

### 3.2.3 Pure and Yb<sup>3+</sup>-doped CdS

Pure and Yb<sup>3+</sup>-doped CdS nanoparticles were prepared according to the following mechano-chemical reaction in a planetary ball mill [10], [11]:

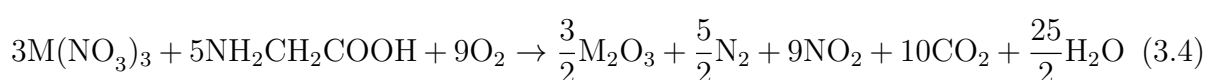


The starting materials were CdCl<sub>2</sub>, YbCl<sub>3</sub>, Na<sub>2</sub>S and NaCl. Milling was performed under high purity argon atmosphere using hardened steel vials and balls, a ball to sample mass ratio of 20:1 and 300 rpm. NaCl was used as diluents in order to prevent nanoparticles aggregation and has little effect on the obtained particles size. The particle size of the product depends on the size of the starting reactants; smaller Na<sub>2</sub>S particles give rise to smaller CdS nanocrystals [12]. In this sense, the mixture Na<sub>2</sub>S + 10NaCl was initially milled for 1 hour. Then, CdCl<sub>2</sub> was added and the mixture was milled for another

hour. The as-obtained powders were washed with distilled water, filtered and dried under vacuum in order to remove NaCl contents.

### 3.3 Combustion reaction

$Y_2O_3$  nanocrystals doped with different  $Er^{3+}$  and  $Yb^{3+}$  concentrations were synthesized following the glycine-nitrate solution combustion reaction:



where  $M = Y^{3+}$ ,  $Er^{3+}$  or  $Yb^{3+}$  [13], [14], [15]. The experimental procedure was as follows: yttrium, ytterbium, erbium nitrates and glycine were mixed in an appropriate ratio and dissolved in distilled water to form the precursor solution. This solution was concentrated by heating in a quartz crucible or in a pyrex beaker on a heating plate. When excess water was evaporated, a spontaneous ignition took place and the combustion reaction was finished originating the oxide nanoparticles (fig. 3.2).



Figure 3.2: Different sequences during the combustion synthesis of RE-doped  $Y_2O_3$  nanoparticles at the Inorganic Chemistry laboratory, University of Cantabria.

The combustion temperature has a great influence on the final particle size, and this reaction temperature can be controlled by changing the glycine-to-nitrates ratio (G/N). For the preparation of RE oxides, it has been reported that lower temperature leads to smaller size for the obtained nanoparticles [15]. In this sense, a G/N lower than stoichiometric,  $G/N=1$ , was used in order to get as small nanoparticles as possible.

In the described process,  $Y_2O_3$  nanocrystals adsorb part of the  $H_2O$  and  $CO_2$  molecules produced during the reaction. The presence of these groups on the nanoparticles surface

yields higher energy phonons which make multiphonon relaxation much more probable, and are responsible for the reduction in the luminescence (see Section 5.2.1). Different heat treatments were carried out in order to reduce the amount of  $\text{OH}^-$  and  $\text{CO}_3^{2-}$  ions which were analyzed by IR absorption spectroscopy. All samples were fired at different temperatures for different periods of time. It must be considered that longer treatments at higher temperatures reduce surface contamination, but they can also induce nanoparticles aggregation with the resulting increase in size.

### 3.4 Pechini's method (sol-gel)

GGG and YAG nanocrystalline powders co-doped with  $\text{Tb}^{3+}$  or  $\text{Eu}^{3+}$  and  $\text{Yb}^{3+}$ , and  $\text{Cr}^{3+}$ -doped GGG nanoparticles have been prepared using the sol-gel Pechini's method as described in Ref. [16]. Among the sol-gel procedures, the preparation of oxides using the formation of an intermediate precursor polyester was proposed by Pechini in 1960's [1]. This technique was initially proposed to prepare niobates and titanates ceramic materials or thin films. Pechini's method is based on the ability of some  $\alpha$ -hydroxycarboxylic acids, such as citric acid (CA), to form chelates between the metal ions (Gd, Ga, Y or Al in our case) and the acid. When this complex is mixed with some polyhydroxyl alcohol, usually polyethylene glycol (PEG), and is heated, the polymerization process takes place. Finally, the polymeric matrix is thermally decomposed to remove the organic groups and form the stoichiometric oxide phase [17].

In our case, the synthesis of ternary oxides according to this method was as follows: First, the precursor solution was prepared by dissolving the nitrates in distilled water and adding a suitable amount of CA, according to the ratio  $\text{CA moles} = 2 \times \text{Nitrates moles}$ . The starting materials were reagent grade  $\text{Gd}(\text{NO}_3)_3$ ,  $\text{Ga}(\text{NO}_3)_3$  and  $\text{Ln}(\text{NO}_3)_3$  or  $\text{Cr}(\text{NO}_3)_3$  for the GGG samples and  $\text{Y}(\text{NO}_3)_3$ ,  $\text{Al}(\text{NO}_3)_3$  and  $\text{Ln}(\text{NO}_3)_3$  in the case of the YAG samples. Then, the solution was heated at  $90^\circ\text{C}$  under stirring until a transparent solution was obtained. At this step, molecules between metal ions and acid are formed. Afterwards, PEG was added to the solution according to  $\text{PEG moles} = \text{CA moles} / 20$  and it was stirred for 15 minutes so that polymerization could take place. Finally, the obtained sol was heated at  $90^\circ\text{C}$  for 24 hours in order to form the gel, an amorphous

mixture of oxides, and this gel was fired at 800 °C for 16 hours to induce its crystallization and to form GGG and YAG nanoparticles (Fig. 3.3).



Figure 3.3: Sol, gel, and powder steps during the GGG and YAG nanoparticles synthesis by Pechini's method at the Biotechnology Department, University of Verona.

### 3.5 Nanoparticles coating

Recently, the fabrication of core-shell structures has attracted increasing attention. Initially, the idea of surface modification was applied in semiconductor nanoparticles but it has also been extended to inorganic luminescent systems [18], [19], [20]. The formation of core-shell structures is an effective way to improve luminescence efficiency since the shell protects the core from interaction with the surrounding medium [21]. Moreover, in some cases such as  $\text{SiO}_2$ , the coating allows the nanocrystals to be redispersible in organic solvents.

A system of chemical reactions to control the growth of spherical silica particles with sizes in the range 50-200 nm was developed by Stöber in 1968 [22]. A procedure to incorporate radioactive isotopes into silica particles was also established by Flachsbart and Stöber [2]. This technique allows the control of the spherical shape for the nanoparticles, and it was used for the  $\text{SiO}_2$  coating of  $\text{Eu}^{3+}$  doped YAG and  $\text{Y}_2\text{O}_3$  [20], [23].

In this work,  $\text{SiO}_2$ -coated nanoparticles were obtained from the above  $\text{Y}_2\text{O}_3$ , GGG and YAG samples using the Stöber method [23], [2]. The experimental details were as follows: a nanopowder sample (0.153 g) was mixed with 60 ml of isopropyl alcohol in a 100 ml flask. The nanoparticles were dispersed with ultrasonic oscillation for 45 minutes. Then, 4.5 ml of deionized water and 6 ml of hydrous ammonia were gradually added under stirring at 50 °C for 10 minutes. After that, 145  $\mu\text{l}$  of tetraethyl orthosilicate (TEOS) was

added and the solution was stirred at 50 °C for 1 hour. Finally, the reaction mixture was centrifuged at 4000 rpm for 10 minutes. The resulting nanoparticles were washed three times by centrifuging in deionized water at 4000 rpm for 10 minutes and dried at 90 °C for 20 hours.

## 3.6 Precipitation method

Different procedures have been reported for the synthesis of LMA, such as solid state reactions [24], a Pechini sol-gel procedure [25], combustion synthesis [26] or a precipitation method [27]. All these methods are known to produce LMA powders with grain size in the range of micrometers. In this work, several attempts to prepare LMA host material by intimately mixing the starting oxides,  $\text{La}_2\text{O}_3 + 2\text{MgO} + 11\text{Al}_2\text{O}_3$ , and heating up to 1400 °C were performed, but a mix of the initial oxides or an amorphous phase was obtained. Another problem related to the synthesis of this system was the presence of  $\text{Al}_2\text{O}_3$  as a non-desired impurity. Combustion synthesis was supposed to give rise to single phase LMA since it requires lower temperatures. However, our experience is that after a combustion reaction and a heat treatment at 500 °C, an amorphous phase was achieved. Firing the samples at 1200 °C for more than ten hours was needed in order to obtain crystalline LMA by combustion. LMA synthesis following the precipitation method was also performed.

Both methods, combustion and precipitation, led to the formation of crystalline LMA with traces of  $\text{Al}_2\text{O}_3$  impurities; but, as we will see later (see Section 5.3.1), luminescence properties are much more interesting for precipitation samples. Therefore, the synthesis of microcrystalline powders of LMA co-doped with different concentrations of  $\text{Mn}^{2+}$  and  $\text{Yb}^{3+}$  was developed in this work following the precipitation method described in Ref. [27]. Stoichiometric quantities of  $\text{La}(\text{NO}_3)_3 \cdot 5\text{H}_2\text{O}$ ,  $\text{Al}(\text{NO}_3)_3 \cdot 9\text{H}_2\text{O}$ ,  $\text{Mg}(\text{NO}_3)_2 \cdot 6\text{H}_2\text{O}$ ,  $\text{Mn}(\text{NO}_3)_2 \cdot \text{H}_2\text{O}$  and  $\text{Yb}(\text{NO}_3)_3 \cdot 5\text{H}_2\text{O}$  were dissolved in distilled water under stirring. Then,  $\text{NH}_4\text{OH}$  was added dropwise until a pH of 8.5 was reached and precipitation as hydroxides occurred. The obtained hydroxides were centrifuged at 3000 rpm for 5 minutes, washed with distilled water, and heated at 90 °C for 20 hours. A treatment at 700 °C for 2 hours and 1500 °C for 1 hour was carried out to obtain the material in its final form.

### 3.7 Colloidal semiconductor nanocrystals

The optical and magnetic properties of wide-gap diluted magnetic semiconductors (DMSs) are attracting broad interest in both fundamental and applied research areas [28]. Two different methods were used for the synthesis of colloidal W-ZnO nanoparticles doped with TM ions such as  $\text{Co}^{2+}$  or  $\text{Mn}^{2+}$ , and W-CoO nanocrystals.

Pure ZnO and  $\text{Zn}_{1-x}\text{TM}_x\text{O}$  with  $x < 30\%$  for Co and  $x < 2\%$  for Mn QDs were prepared using hydrolysis and condensation of acetates ( $(\text{OAc})_2$ ) solution in dimethyl sulfoxide (DMSO) [29], [30]. The experimental procedure was as follows: Acetates were dissolved in DMSO, typically  $9 \cdot 10^{-3}$  moles of  $\text{Zn}(\text{OAc})_2$  and  $\text{Co}(\text{OAc})_2$  or  $\text{Mn}(\text{OAc})_2$  in 90 ml of DMSO. Simultaneously, tetramethyl ammonium hydroxide ( $\text{N}(\text{Me})_4\text{OH}$ ) (1.8 equiv of  $\text{OH}^-$ ) was dissolved in 30 ml of ethanol. Then, the  $\text{N}(\text{Me})_4\text{OH}$  solution was added dropwise to the  $(\text{OAc})_2$  in DMSO under constant stirring and the reaction took place. After a rapid nucleation, the reaction Ostwald ripens, which means that small crystals are unstable and shrink due to their large surface-to-volume ratio while larger particles are stable and grow [31]. The reaction time and the addition of  $\text{N}(\text{Me})_4\text{OH}$  are important factors in this synthesis. Bigger nanoparticles were obtained for longer reaction times. When  $\text{Co}(\text{OAc})_2$  or  $\text{Mn}(\text{OAc})_2$  concentration increases, more time is needed, not only for the reaction to occur, but also for the nanoparticles to grow. Dopants are excluded from the initial nucleation but are incorporated into the ZnO nanoparticles almost isotropically during growth from solution. The formation of ZnO becomes linear with base addition above 1.0 equiv of  $\text{OH}^-$ . Figure 3.4. shows the sequence of a reaction flask during the synthesis of a  $\text{Co}^{2+}$ -doped ZnO sample. The first image, before the base addition, shows the characteristic pink color of octahedral  $\text{Co}^{2+}$  in  $(\text{OAc})_2$ .  $\text{N}(\text{Me})_4\text{OH}$  addition turns the solution from pink to blue, indicating the tetrahedral coordination of  $\text{Co}^{2+}$  in ZnO. Nanocrystals prepared by this method were precipitated in ethyl acetate, washed with ethanol and precipitated again by adding heptane. Colloidal nanocrystals were usually stabilized by a layer of surfactants attached to their surface. The energy with which surfactant molecules adhere to the surfaces of growing nanocrystals is one of the most important parameters influencing crystal growth. Murray *et al.* discussed this fact for

the growth of CdSe nanoparticles capped with trioctylphosphine oxide (TOPO) [32]. For the final capping treatment, melted TOPO was added to the nanocrystals and heated at 180 °C for 30 minutes. The resulting powders were precipitated in ethanol or methanol and resuspended in toluene.



Figure 3.4: Preparation of ZnO: Co<sup>2+</sup> colloidal nanocrystals at the Chemistry Department, University of Washington. The solution changes from pink to blue indicating the conversion of octahedral Co<sup>2+</sup> to tetrahedral Co<sup>2+</sup>.

Colloidal W-CoO nanoparticles were synthesized using a nonaqueous solution method with the reaction system composed by the metal fatty acid salt, the corresponding fatty acid and a hydrocarbon solvent [33], [30]. For preparing CoO nanoparticles, cobalt stearate (Co(St)<sub>2</sub>) (0.625 g) was used as the precursor, a certain amount of stearic acid (0.305 g) was employed as ligands and octadecene (ODE) (5 g) was chosen as the non-coordinating solvent. Co(St)<sub>2</sub> and stearic acid were dissolved in ODE stirring at 120 °C under vacuum. When the purple mixture was fully dissolved, it was placed in a N<sub>2</sub> flow, and it was rapidly heated to 320 °C and held there under stirring for 1 hour. When the solution turned greenish W-CoO nanocrystals were formed. After cooling to 100 °C, the obtained CoO particles were precipitated with ethanol, capped with TOPO, precipitated in acetone and suspended in toluene.

# Bibliography

- [1] M.P. Pechini. U.S.A. Patent 3.330.697. 1967.
- [2] H. Flachsbart and W. Stöber. Preparation of Radioactively Labeled Monodisperse Silica Spheres of Colloidal Size. *J. Colloid Interface Sci.*, **30**: 568–573, 1969.
- [3] C.C. Koch. Synthesis of nanostructured materials by mechanical milling: Problems and oportunities. *Nanostruct. Mater.*, **9**: 13–22, 1997.
- [4] S.R. Mishra, G.J. Long, F. Grandjean, R.P. Hermann, S. Roy, N. Ali, and A. Viano. Magnetic properties of iron nitride-alumina nanocomposite materials prepared by high-energy ball milling. *Eur. Phys. J. D*, **24**: 93–96, 2003.
- [5] V.V. Boldyrev. Mechanochemistry and mechanical activation of solids. *Solid State Ionics*, **63-65**: 537–543, 1993.
- [6] S. Mørup, J.Z. Jiang, F. Bødker, and A. Horsewell. Crystal growth and the steady-state grain size during high-energy ball-milling. *Europhys. Lett.*, **56**: 441–446, 2001.
- [7] R.E. Thoma, G.M. Hebert, H. Insley, and C.F. Weaver. Phase equilibria in the System Sodium Fluoride-Yttrium Fluoride. *Inorg. Chem.*, **2**: 1005–1012, 1963.
- [8] N. Martin, P. Boutinaud, R. Mahiou, J.C. Cousseins, and M. Bouderbala. Preparation of fluorides at 80 °C in the NaF(Y, Yb, Pr)F<sub>3</sub> system. *J. Mater. Chem.*, **9**: 125–128, 1999.
- [9] J. Lu, Q. Zhang, and F. Saito. Mechanochemical Synthesis of Nano-sized Complex Fluorides from Pair of Different Constituent Fluoride Compounds. *Chem. Lett.*, **1**: 1176–1177, 2002.

- 
- [10] T. Tsuzuki and P.G. McCormick. Mechanochemical synthesis of metal sulphide nanoparticles. *Nanostruct. Mater.*, **12**: 75–78, 1999.
- [11] T. Tsuzuki and P.G. McCormick. Synthesis of CdS quantum dots by mechanochemical reaction. *Appl. Phys. A*, **65**: 607–609, 1997.
- [12] T. Tsuzuki, J. Ding, and P.G. McCormick. Mechanochemical synthesis of ultrafine zinc sulfide particles. *Physica B*, **239**: 378–387, 1997.
- [13] J.A. Capobianco, F. Vetrone, J.C. Boyer, A. Speghini, and M. Bettinelli. Enhancement of Red Emission via Upconversion in Bulk and Nanocrystalline Cubic  $\text{Y}_2\text{O}_3$ :  $\text{Er}^{3+}$ . *J. Phys. Chem. B*, **106**: 1181–1187, 2002.
- [14] J.A. Capobianco, F. Vetrone, T. D’Alessio, G. Tessari, A. Speghini, and M. Bettinelli. Optical spectroscopy of nanocrystalline cubic  $\text{Y}_2\text{O}_3$ : Er obtained by combustion synthesis. *Phys. Chem. Chem. Phys.*, **2**: 3203–3207, 2000.
- [15] T. Ye, Z. Guiwen, Z. Weiping, and X. Shangda. Combustion synthesis and photoluminescence of nanocrystalline  $\text{Y}_2\text{O}_3$ : Er phosphors. *Mater. Res. Bull.*, **32**: 501–506, 1997.
- [16] M. Daldosso, D. Falcomer, A. Speghini, P. Ghigna, and M. Bettinelli. Synthesis, EXAFS investigation and optical spectroscopy of nanocrystalline  $\text{Gd}_3\text{Ga}_5\text{O}_{12}$  doped with  $\text{Ln}^{3+}$  ions ( $\text{Ln}=\text{Eu}, \text{Pr}$ ). *Opt. Mat.*, **30**: 1162–1167, 2008.
- [17] A.V. Rosario and E.C. Pereira. The effect of composition variables on precursor degradation and their consequence on  $\text{Nb}_2\text{O}_5$  film properties prepared by the Pechini Method. *J. Sol-Gel Sci. Techn.*, **38**: 233–240, 2006.
- [18] J.S. Steckel, J.P. Zimmer, S. Coe-Sullivan, N.E. Stott, V. Bulovic, and M.G. Bawendi. Blue Luminescence from (CdS)ZnS Core-Shell Nanocrystals. *Angew. Chem.*, **116**: 2206–2210, 2004.
- [19] O. Lehmann, K. Kömpe, and M. Haase. Synthesis of  $\text{Eu}^{3+}$ -Doped Core and Core/Shell Nanoparticles and Direct Spectroscopic Identification of Dopant Sites at

- the Surface and in the Interior of the Particles. *J. Am. Chem. Soc.*, **126**: 14935–14942, 2004.
- [20] D. Hreniak, P. Psuja, W. Stręk, and J. Hölsä. Luminescence properties of  $\text{Y}_3\text{Al}_5\text{O}_{12}$ :  $\text{Eu}^{3+}$ -coated submicron  $\text{SiO}_2$  particles. *J. Non-Cryst. Solids*, **354**: 445–450, 2008.
- [21] P. Zhu, Q. Zhu, H. Zhu, H. Zhao, B. Chen, Y. Zhang, X. Wang, and W. Di. Effect of  $\text{SiO}_2$  coating on photoluminescence and thermal stability of  $\text{BaMgAl}_{10}\text{O}_{17}$ :  $\text{Eu}^{2+}$  under VUV and UV excitation. *Opt. Mat.*, **30**: 930–934, 2008.
- [22] W. Stöber, A. Fink, and E. Bohn. Controlled Growth of Monodisperse Silica Spheres in the Micron Size Range. *J. Colloid Interface Sci.*, **26**: 62–69, 1968.
- [23] Q. Lü, A. Li, F. Guo, L. Sun, and L. Zhao. The two-photon excitation of  $\text{SiO}_2$ -coated  $\text{Y}_2\text{O}_3$ :  $\text{Eu}^{3+}$  nanoparticles by a near-infrared femtosecond laser. *Nanotech.*, **19**: 205704–205712, 2008.
- [24] W. Ge, H. Zhang, J. Wang, D. Ran, S. Sun, H. Xia, J. Liu, X. Xu, X. Hu, and M. Jiang. Growth and thermal properties of  $\text{Co}^{2+}$ :  $\text{LaMgAl}_{11}\text{O}_{19}$  crystal. *J. Crystal Growth*, **282**: 320–329, 2005.
- [25] P.Y. Jia, M. Yu, and J. Lin. Sol–gel deposition and luminescent properties of  $\text{LaMgAl}_{11}\text{O}_{19}$ :  $\text{Ce}^{3+}/\text{Tb}^{3+}$  phosphor films. *J. Solid State Chem.*, **178**: 2734–2740, 2005.
- [26] S. Ekambaram, K.C. Patil, and M. Maaza. Synthesis of lamp phosphors: facile combustion approach. *J. Alloys Compd.*, **393**: 81–92, 2005.
- [27] J.M.P.J. Verstegen, J.L. Sommerdijk, and J.G. Verriet. Cerium and Terbium luminescence in,  $\text{LaMgAl}_{11}\text{O}_{19}$ . *J. Lumin.*, **6**: 425–431, 1973.
- [28] J.M.D. Coey. Dilute magnetic oxides. *Curr. Opin. Solid State Mater. Sci.*, **10**: 83–92, 2006.

- 
- [29] D.A. Schwartz, N.S. Norberg, Q.P. Nguyen, J.M. Parker, and D.R. Gamelin. Magnetic Quantum Dots: Synthesis, Spectroscopy, and Magnetism of  $\text{Co}^{2+}$ - and  $\text{Ni}^{2+}$ -doped ZnO Nanocrystals. *J. Am. Chem. Soc.*, **125**: 13205–13218, 2003.
- [30] M.A. White, S.T. Ochsenbein, and D.R. Gamelin. Colloidal Nanocrystals of Wurtzite  $\text{Zn}_{1-x}\text{Co}_x\text{O}$  ( $0 \leq x \leq 1$ ) : Models of Spinodal Decomposition in an Oxide Diluted Magnetic Semiconductor. *Chem. Mater.*, **20**: 7107–7116, 2008.
- [31] Y. Yin and A.P. Alivisatos. Colloidal nanocrystal synthesis and the organic-inorganic interface. *Nature*, **437**: 664–670, 2005.
- [32] C.B. Murray, D.J. Norris, and M.G. Bawendi. *J. Am. Chem. Soc.*, **115**: 8706–8715, 1993.
- [33] N.R. Jana, Y. Chen, and X. Peng. Size- and Shape-Controlled Magnetic (Cr, Mn, Fe, Co, Ni) Oxide Nanocrystals via a Simple and General Approach. *Chem. Mater.*, **16**: 3931–3935, 2004.